Journal of Ovarian Research

RESEARCH

Open Access

RLIP depletion suppresses ovarian cancer growth and metastasis

B. Madhu Krishna[1], Pankaj Garg[2], David Horne[3], Prakash Kulkarni[1], Ravi Salgia[1] and Sharad S. Singhal[1*]

Abstract

One of the leading causes of cancer deaths worldwide is ovarian tumor metastasis. It is very common for ovarian cancer (OC) cells to metastasize to the peritoneum. Free-floating OC cells can drift in the ascitic fluid (fluid that accumulates in the abdominal cavity due to cancer) and attach to the peritoneal lining of the abdominal cavity. In OC, peritoneal metastasis is strongly associated with poor prognosis. This study compared the effects of RLIP inhibition in various OC cell lines and in an orthotopic mouse model of ovarian metastasis to assess its anti-proliferative and anti-metastatic activity. Relative to the control treatment, RLIP inhibition and/or depletion decreased in vitro cell viability and minimized migratory and invasive capabilities of OC cells. The in vivo model was performed using HeyA8 OC cells expressing the luciferase gene that were implanted into the mice followed by the treatment of the mice with RLIP antisense (RAS, 4 mg/kg, b.w.), RLIP antibody (Rab, 4 mg/kg, b.w.) and a combination of RLIP antisense and RLIP antibody (RAS + Rab). Primary tumor weight and metastatic lesions were reduced in both RAS-treated and Rab-treated mice compared to control mice. Mice that received the RAS + Rab combination had almost no metastasis, and their tumor weight was much lower than that seen with either agent alone. Survival was also extended in NSG mice inoculated with HeyA8-luc OC cells when treated with RLIP-targeting agents. Overall, our findings indicate that RLIP antisense together with RLIP antibodies may be effective in controlling primary tumor growth and peritoneal metastasis, supporting the need for continued investigation.

Highlights

Key findings of this study with potential clinical relevance include:

- RLIP is an attractive therapeutic target with the ability to suppress human OC at multiple stages of development.
- Reducing RLIP levels significantly inhibits OC cell growth and enhances apoptosis compared with controls.
- RLIP blockade/depletion may serve as a broad-spectrum therapeutic strategy that remains effective regardless of common pathway differences among OC subtypes.
- This is the first evidence from integrated in vitro and in vivo studies demonstrating the strong therapeutic promise of RLIP-targeting agents for treating metastatic OC.

Keywords RLIP, Ovarian cancer, Antisense, Glutathione-conjugates, Mercapturic acid pathway, Metastasis, Chemotherapeutics, Orthotopic mouse model

*Correspondence:
Sharad S. Singhal
ssinghal@coh.org
[1]Department of Medical Oncology and Therapeutic Research, Beckman Research Institute, City of Hope Comprehensive Cancer Center, National Medical Center, 1500 E Duarte Road, Duarte, CA 91010, USA
[2]Department of Chemistry, GLA University, NH-19, Mathura-Delhi Road, Mathura, Uttar Pradesh 281406, India
[3]Department of Molecular Medicine, Beckman Research Institute, City of Hope Comprehensive Cancer Center, and National Medical Center, 1500 E Duarte Road, Duarte, CA 91010, USA

One sentence summary

We demonstrate that RLIP is prerequisite for ovarian cancer initiation, is expressed at significantly higher levels in ovarian cancer cells compared with non-malignant cells, and its depletion or inhibition effectively suppresses ovarian carcinogenesis and metastases.

Introduction

Ovarian cancer (OC) is a severe disease characterized by the uncontrolled proliferation of ovarian cells. Its symptoms are often vague or unnoticeable in the early stages, making early detection difficult [1–4]. OC is among the most lethal gynecological cancers, due to delayed diagnosis often gets diagnosed at advanced stages, which limited therapeutic options leading to poor survival rates [4–6]. Its etiology is diverse and may involve hereditary factors, reproductive history, and hormonal influences, which highlights the need for broad risk-assessment and screening strategies [7].

OC is considered the deadliest gynecologic cancer and is marked by numerous genetic mutations that drive uncontrolled cell growth and division. More than 95 out of 100 cases are epithelial ovarian cancers (EOCs), while non-epithelial OCs account for less than 5 cases out of 100 [1, 7–10]. The peritoneum and omentum, the lining and fatty tissue of the abdominal cavity, are the most common metastatic sites. Peritoneal metastasis is a major cause of death in OC. Unlike many cancers that spread mainly through the blood or lymphatic systems, OC cells often detach from the primary tumor, float in the ascitic fluid of the abdominal cavity, and then adhere to peritoneal surfaces, especially the omentum.

Ral-interacting/binding protein (RLIP; 18p11.22: *RALBP1*) has become an important target in cancer therapy due to its elevated expression in many cancer cell lines and tumor tissues [11–15]. RLIP is a versatile protein localized across the plasma membrane, cytosol, and nucleus, and is closely linked with the growth of solid tumors. RLIP significantly contributes to tumor progression and is abundantly expressed across multiple tissues, including the ovary. RLIP plays crucial role in cancer cell migration, invasion in surrounding tissues, and metastasis through modulating endocytosis, cytoskeletal dynamics, and stress-protective transport. These processes facilitate cancer cells to achieve decisive migratory and survival capabilities during metastatic progression. RLIP is obligatory for clathrin-dependent endocytosis of receptor tyrosine kinases, inclusive of growth factor receptors. This process modulates duration and intensity of downstream pro-survival and proliferative signaling cascades, such as Akt pathway, thereby enabling cancer cells to produce sustained oncogenic signal that promote tumor cell survival and growth. Earlier studies showed that RLIP knockout homozygous ($RLIP^{-/-}$) mice demonstrated that angiogenesis and early tumor neovascularization depended on RLIP. Pro-angiogenic factors regulated by RLIP include vascular endothelial growth factor (VEGF) and hypoxia-inducible factor-1 (HIF-1) [13, 16].

The endogenous metabolites and environmental toxins are converted into glutathione (GSH)-electrophile conjugates (GS-Es), which are then transported by an ATP-dependent, non-ABC transporter known as RLIP [17–20]. It is also important that RLIP is required in the growth of tumors as well as metastasis in melanomas [21], non-small cell lung cancer [22, 23], renal cell carcinoma [24], and ovarian carcinomas [25–27]. RLIP knockdown by means of small interfering RNA (siRNA) has been demonstrated to inhibit tumor growth and metastasis in prostate cancer xenografts [28]. Likewise, in UMUC3 cells, RLIP knock down using lentiviral vectors resulted in reduced metastasis of lung cancer in a bladder cancer xenograft model [13]. These results have established the substantial role of RLIP in tumorigenesis and cancer cell motility.

The objective of the present study is to examine the effect of RLIP inhibition or depletion on the anti-migratory and anti-metastatic properties of OC cell lines in both in vitro and in vivo systems. We assessed the anti-migratory and anti-invasive actions of RLIP-targeting agents in OC cell lines in vitro. Additionally, we evaluated the anti-metastatic effects of RLIP depletion/inhibition using antisense and antibody treatments in an orthotopic mouse OC model after intraperitoneal injection of HeyA8 OC cells expressing luciferase. Our results show that RLIP-targeting agents reduce the motility and downstream signaling pathways of OC cells, suggesting that RLIP-targeting may be a promising approach for OC treatment.

Materials and methods

Materials

Details regarding the procurements and specifications of all the chemicals and biochemicals used in this study were already summarized in our previous publication [27].

Cell lines and culture conditions

A2780, HeyA8, and SKOV3 human OC cell lines were generous gifts of Dr. Edward Wang (City of Hope, Duarte, CA). Dr. Fiemu Nwariaku (UT Southwestern Medical Center, Dallas, TX) was also a source of HUVECs and HAVSMCs. OC cells were cultured using RPMI-1640 medium at 37 °C and 5% CO_2. EGM-2 was used to keep HUVECs, and DMEM was used to maintain HAVSMCs. Each of the media was supplemented with heat inactivated 10% FBS with 1% penicillin streptomycin solution. The genomics core facility at the City of Hope

National Medical Center performed Short tandem repeat (STR) profiling for cell line authentication. Screening for mycoplasma contamination was done at a regular interval of every three months as a measure to ensure culture integrity.

Luciferase transfection

HeyA8 and A2780 cells were transduced with a lentiviral luciferase construct under the EF1α promoter (pLVX-EF1alpha-Luc-PGK-Puro). Transduced cells were selected using puromycin for seven days. Each cell line was cloned three times, expanded, and luciferase activity was confirmed using the Promega Firefly Luciferase Assay Kit (Cat #E1500).

RLIP antisense preparation

DNA was modified with phosphorothioate groups targeting amino acid sites of RLIP (171–185 and 510–555) to improve nuclease resistance. BLAST analysis was performed to verify specificity against the RLIP gene. Phosphorothioate DNA (desalted) was bought from Biosynthesis Inc. (Lewisville, TX). Nucleotides 507–527 of RLIP cDNA (AAGAAAAAGCCAATTCAGGAGCC), a 21-nt antisense sequence, were validated and complemented with the phosphorothioate antisense sequence (GGCTCCTGAATTGGCTTTTTC). A scrambled sequence (CATCGAAATCGTTGCAGTTAC) served as the negative control. Gene silencing was assessed after 24–48 h of transfection using Maxfect Transfection Reagent (MoleculA).

Isolation of crude membrane fractions from mouse tissues

Crude membrane fractions were isolated either by gravity after flotation of the full suspension with flocculant polymers, or by centrifugation following filtration of the suspension with flocculant polymers. All steps were performed at 4 °C unless stated otherwise. Blood contamination was minimized by perfusing tissues with PBS using a 22-gauge syringe. Tissue homogenates (20% w/v) were prepared in Tris-HCl buffer (10 mM, pH 7.4) containing 1.4 mM 2-mercaptoethanol. Homogenates from tumors, liver, ovary, kidney, brain, and spleen were centrifuged at 8,000 × g for 45 min. Supernatants were further centrifuged by ultracentrifugation at 100,000 × g for 60 min to obtain membrane pellets. Pellets were solubilized in lysis buffer (10 mM Tris-HCl, pH 7.4; 0.5 mM BHT; 0.1 mM PMSF; 0.1 mM EDTA; 1.4 mM β-mercaptoethanol) with 0.5% polidocanol. Samples were sonicated (50 W, 30 s, 4 °C) followed by intermittent shaking for 4 h and centrifuged again at 100,000 × g for 2 h. The supernatant was carefully extracted and stored for further studies.

ELISA-based quantification of RLIP depletion

The depletion of RLIP was determined by ELISA-based assays on cellular and tissue samples. Although RLIP purification is the most accurate way of analyzing the product of analysis, ELISA protocols of crude homogenate are a feasible substitute. Flat bottom 96-well plates were coated with carbonate-bicarbonate buffer solution (pH 9.6) that contained 1% BSA and 0.01% Tween 20 and were incubated at 37 °C for 2 h. This was followed by loading each well with protein solution (0.1–4 µg in100 µl/well) in the same buffer and incubation at 37 °C for another 2 h. Blocking was done after mixing out the reactant solution and subsequently, 100 µl of 10% goat serum at room temperature was added and incubate for 30 min. Each well was wetted with 100 µg/mL primary antibody of RLIP and incubated for 2 h at 4 °C followed by washing with 1x PBST (PBS-Tween) buffer. After that, each well was flooded with100 µl of secondary antibody and incubated at 37 °C for 30 min. Upon further 1x PBST washing, each well was wetted with 100 µl of HRP solution and incubated on a shaker to 10–20 min left this to incubate to allow for detection. The ELISA plate reader recorded the absorbance after 405 nm using a standard reference curve made with purified recombinant RLIP protein [27].

MTT cell viability assay

The effects of RLIP depletion on cell survival through all OC cell lines A2780, HEYA8, SKOV3, and normal cells HAVSMC, HUVEC were measured in the MTT assay. According to manufacture specifications Maxfect Transfection Reagent (MoleculA, Inc.) was used to perform transfection with RLIP antisense (0–10 µg/ml) in plates containing 5,000 cells per well. After 48 h, cells in each well were administrated with 10 µl of 5 mg/mL MTT solution and plates were incubated for 4 h at 37 °C. Upon observing formazan crystals under microscope, medium with testing solution was aspirated, and formazan crystals were dissolved using 100 µl DMSO following PBS washing. Absorbance was measured at a wavelength of 570 nm and 630 nm (background) using Microplate XMark spectrophotometer from Bio-Rad, Hercules, CA. The ratio of background-subtracted absorbance values of treated samples to untreated controls was used to calculate the percentage of cell survival. Three separate experiments, each with four technical replicates per condition ($n = 12$), are used to present the data as mean ± standard deviation. The RLIP reduction, which occurred as a consequence of the effects of antisense treatment, was verified by western blot.

Colony formation assay

Effect of RLIP antisense on colony formation was determined by incubating 0.1×10^6 cells with 10 µg/ml RLIP

antisense or scrambled antisense for 48 h in 500 µl. Aliquots (50 or 100 µL) of 4 ml cell suspension were plated using a 60 mm petri dish. The cells were incubated for 7 days, after which they were fixed and stained with 0.5% of methylene blue for 30 min. Results were counted in the Alpha Innotech Alpha Imager HP system [27].

Cell migration assay

Wound healing assay was employed to investigate the effect of RLIP antisense on the migratory phenotype of SKOV3 and HeyA8-luc OC cells. Cells were seeded in 6-well discs and allowed to reach approximately 90% confluence. A line of cell monolayer wounding was produced with a 10 µl sterile pipette tip. Cellular debris in each well were carefully eliminated with PBS, cells inoculated with medium without FBS and were exposed to 10 µg/ml of either control scrambled (CAS) or RLIP antisense (RAS). Close microscopic photographs of the wound were obtained after 0, 12, and 24 h. These photographs were used to assess cell migration capacity. The presented data illustrates mean and standard deviation of three different experiments.

Cell invasion assay

A Transwell Boyden chamber was used to evaluate the in vitro effects of RLIP antisense on the migration of SKOV3 and HeyA8-luc OC cells. Briefly, the OC cells (0.5×10^6 cells/well) were seeded in the upper chamber of 24-well Transwell plates in serum-free medium. Cells were treated with either scrambled control or RLIP antisense at a final concentration of 10 µg/ml for 24 h. The lower chamber was filled with DMEM containing 10% FBS to serve as a chemoattractant. Cell migration was carried out at 37 °C in a humidified incubator with 95% air and 5% CO_2. After incubation, non-migrated cells on the upper surface of the insert were gently removed using a PBS-moistened cotton swab. Migrated cells attached to the lower surface were fixed with 4% paraformaldehyde for 15 min. To visualize the migrated cells, inserts were permeabilized with 0.2% Triton X-100 in PBS, followed by staining with 0.2% crystal violet at room temperature. Images were captured from five randomly selected fields per insert using a light microscope at 200× magnification. After imaging, the stained inserts were rinsed with water, blotted dry, and placed in an empty well. The dye was extracted by adding 200 µl of extraction buffer and incubating the inserts on an orbital shaker for 10 min. Absorbance was measured at 560 nm using a plate reader to quantify the number of invading cells. The percentage of invading cells in the RLIP antisense-treated group relative to the scrambled control was calculated from the absorbance values. All experiments were performed in triplicate.

Orthotopic mouse model of HeyA8-luc OC

Animals were treated according to guidelines on animal care as approved by the institutional Animal Care and Use Committee (IACUC protocol 22011) at City of Hope. The Jackson Laboratory (Sacramento, CA) provided female NOD scid gamma (NSG) mice (8 weeks old with the body weight ranging between 20 and 22 g). The animals were acclimatized one week before the start of study. 25 female NSG homozygous mice were categorized as follows: (**i**) pre-immune serum (PIS); (ii) RLIP antibody (Rab); (iii) control antisense (CAS); (iv) RLIP antisense (RAS); and (v) Rab + RAS (25). HeyA8 OC cells (1×10^6 cells in 0.1 mL of PBS) transfected with the luciferase gene were implanted into NSG mouse peritoneum. After tumor cell inoculation, mice were injected intraperitoneally (*i.p.*) with 3 mg D-luciferin in 0.1 mL of saline and subsequently tested for the presence of tumor cells by bioluminescence imaging using SPECTRAL Lago X Imaging System (Spectral Instruments Imaging, Tucson, AZ). Bioluminescent intensity was measured on the Aura Imaging Software 4.0 created by Spectral Instruments Imaging. Control mice were treated with scrambled antisense (4 mg/kg b.w. *i.p.*) and pre-immune IgG (4 mg/kg b.w. *i.p.*), whereas the test group of mice was treated with RLIP antibodies (4 mg/kg b.w. *i.p.*), RLIP antisense (4 mg/kg b.w. *i.p.*), and a combination of both as described previously [25–27]. Treatment started on Day 3. All groups showed bioluminescence from in-vivo imaging twice a week following peritoneum injection. Weekly records were made on body weights and cross-sectional areas of the primary tumor using a caliper, including a tumor photograph, at week 7 (day 49). Mice were followed daily and euthanized according to the IACUC-approved protocol (signs and symptoms of the cancer [i.e., lost 20% of body weight, dehydration, swelling of the abdomen, and difficulty walking]) and the tumor, ovary, liver, kidney, spleen, and brain tissues were harvested to be examined under the microscope by histopathologic means and molecular analyses. Figure 3 shows representative pictures of mice from each group. At the end of the study (i.e., week 7), asphyxiation using CO_2 and cervical dislocation were used to euthanize the animals. The unpaired Student *t*-test was used to compare the weights of the tumors of the groups.

Immunohistochemical analysis

To determine RLIP expression in vivo, sections of mouse tumors and tissues were fixed overnight with formalin and subjected to embedding in paraffin followed by cutting of sections to 5-µm thick and mounting them on Poly-L-lysine-coated slides. The sections were deparaffinized, rehydrated respectively using xylene and then using graduated ethanol. Hematoxylin and eosin (H and E) staining was used to assess the level of hyperplasia,

followed by immunostaining for E-cadherin and vimentin involved in epithelial-mesenchymal transition (EMT), CD31 to visualize blood vessels, Ki67 and RLIP to assess cell proliferation, and vimentin to analyze mesenchymal cells was performed using a universal avidin/biotin complex detection kit (Vector Laboratories). Immunoreactivity manifested itself in dark brown and non-immunoreactive regions that were considered to be background staining. The samples were photographed using an Olympus DP72 microscope at a magnification of 40×, and the DP2-BSW digital imaging package was used to examine the antigen staining intensity.

Statistical analysis

Unpaired two-tailed Student *t*-tests were used to analyze data, with presented as mean ± standard deviation. Tumor size changes and body weight variations over time were shown using scatter plots. Significant differences between control and treatment groups were determined using ANOVA with post-hoc tests. A *p*-value below 0.05 was considered significant.

Ethics statement

No human participants were employed in this current study. City of Hope approved IACUC protocol for the experiments with all laboratory animals. Mice exhibiting signs of pain, distress, or tumor-associated morbidity were euthanized humanely.

Results

OC cell expression of RLIP

Recent findings revealed that there was a significant rise in the abundance of RLIP in the OC cells relative to the normal cytosol, and the OC cells treated with RLIP antisense confirmed the reduction of RLIP expression (25, 26), implying that RLIP can be a possible target in regulating the growth of OC cells. Table 1 gives the protein content measured as the total crude protein in the membrane of 1×10^8 cells in the log-growth phase. According to this evaluation, the contents of RLIP protein were 12 ± 2 μg/10^8 normal cells and 58 ± 6 μg/10^8 OC cells, making up 0.23% and 0.81% of the total detergent-soluble membrane proteins in normal and OC cells, respectively. The values shown are averages of three independent measurements of three replicates ($n = 9$). These data indicate that the expression of RLIP is significantly greater in OC cells than in cells that are non-malignant (Table 1).

Table 1 RLIP protein in human normal and ovarian cancer cells

	Total crude protein (mg/10^8 cells)	RLIP protein	
		μg/10^8 cells	% of total crude protein
Nonmalignant			
HAVSMC (aorta smooth muscle)	4.96 ± 0.58	13 ± 2	0.26
HUVEC (umbilical endothelial)	5.24 ± 0.46	11 ± 2	0.21
Malignant			
HeyA8-luc	7.14 ± 0.62	58 ± 7	0.81
A2780-luc	6.78 ± 0.48	52 ± 7	0.77
SKOV3	7.62 ± 0.84	66 ± 5	0.86

A homogenate has been extracted from 100×10^6 cells after cell lines had been cultured in the appropriate medium. DNP-SG affinity column chromatography was used to separate RLIP from the total crude membrane fraction, and ELISA was used to quantify [27, 29]. Human umbilical vascular endothelial cells are known as HUVEC, and human aortic vascular smooth muscle cells are known as HAVSMC

RLIP inhibition/depletion down-regulates OC cell viability

The effect of RLIP inhibition on OC cells was studied using RLIP antisense and RLIP antibodies as depletion or inhibitory agents, respectively [21]. Protein-A affinity chromatography was used to isolate the control immunoglobulin fraction of the pre-immune serum. Previous Ouchterlony double immunodiffusion tests had shown that anti-RLIP IgG was non-reactive with other proteins, including Pgp and MRP [29]. Pre-immune IgG (40 μg/ml), anti-RLIP IgG (40 μg/ml), scrambled antisense, or RLIP antisense (10 μg/ml) were incubated with cells for 24 h. A clear growth-inhibitory effect was observed in OC cells treated with RLIP antibodies or RLIP antisense, but not in their respective controls (Fig. 1A). In contrast, non-malignant HAVSMC and HUVEC cells showed no significant changes in growth when exposed to RLIP inhibition or depletion. The impact of RLIP depletion on cell survival and proliferation was further supported by examining the clonogenic potential of OC cells. Colony-forming assays demonstrated that RLIP antisense reduced RLIP levels and decreased the cells' ability to form colonies (Fig. 1B).

RLIP depletion effects migration and invasion of OC cells

RLIP depletion induces in vitro anti-migratory and anti-invasive effects in OC cells. The metastatic cascade involves complex migration and invasion events that allow tumor cells to spread to other organs, even when they originate elsewhere. To examine the effects of RLIP reduction on migration, HeyA8-luc and SKOV3 cells were used in a scratch wound-healing assay and treated with either scrambled or RLIP antisense (10 μg/ml final concentration). At 12 and 24 h, RLIP antisense treatment significantly inhibited the ability of OC cells to migrate (Fig. 2A). Next, we examined the effect of RLIP antisense treatment (10 μg/ml final concentration) on the invasion ability of HeyA8-luc and SKOV3 cells using Matrigel invasion chambers after 24 h. As shown in Fig. 2B, crystal violet staining revealed a marked reduction in the

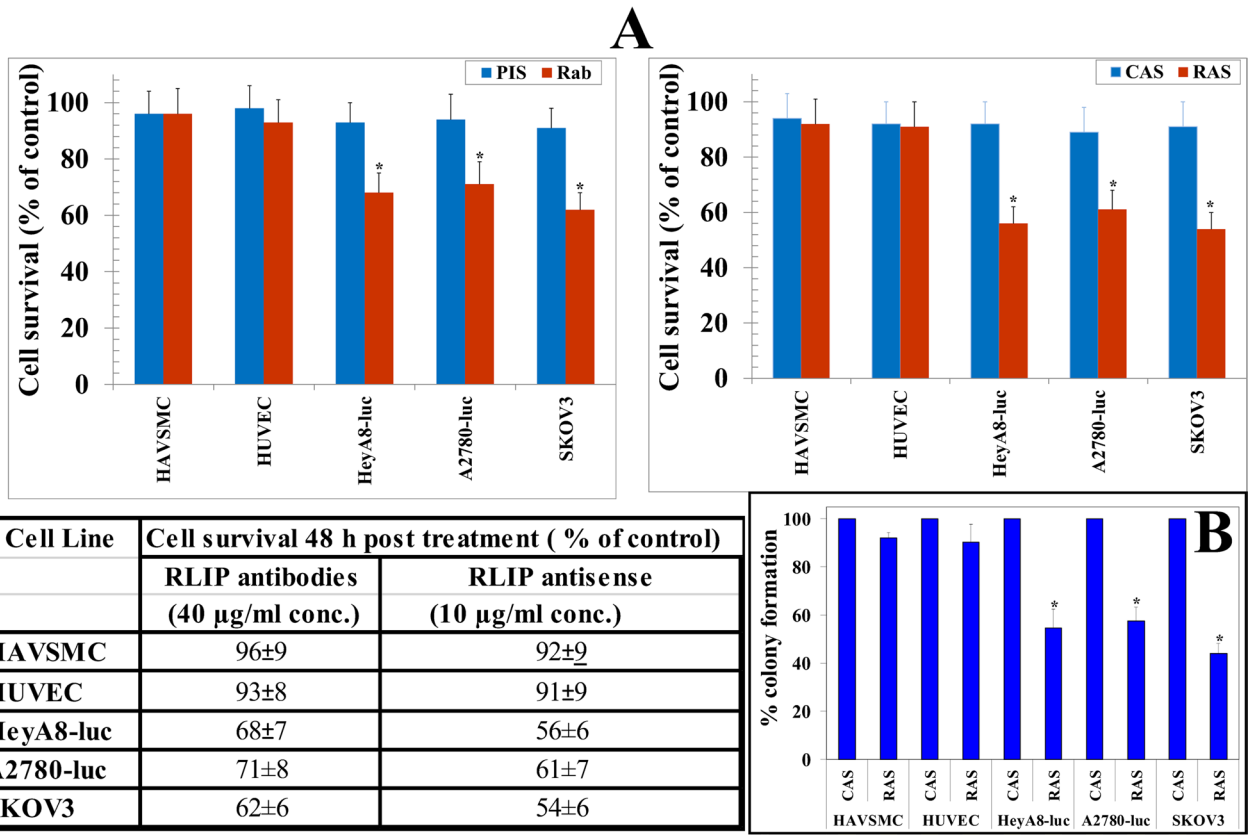

Cell Line	Cell survival 48 h post treatment (% of control)	
	RLIP antibodies (40 µg/ml conc.)	RLIP antisense (10 µg/ml conc.)
HAVSMC	96±9	92±9
HUVEC	93±8	91±9
HeyA8-luc	68±7	56±6
A2780-luc	71±8	61±7
SKOV3	62±6	54±6

Fig. 1 Impact of RLIP antibody and RLIP antisense on normal and OC cells survival. **A** Effect of RLIP antibody (40 µg/ml final concentration) on cell survival was determined by MTT assay. Depletion of RLIP expression by RLIP antisense (10 µg/ml final concentration) was also done using Maxfect Transfection Reagent, according to the manufacturer's instructions. Cell survival was measured by MTT cytotoxicity assay 48 h after treatment. Table represents percent cell survival after RLIP antibodies and RLIP antisense treatment. The values are presented as mean ± SD from three separate determinations with eight-replicates each ($n = 24$). Blue bars, Control treatments; red bars, RLIP-targeting agent treatments. *$p < 0.04$, compared to respective controls. **B** Colony-forming efficiency in OC cells and non-malignant cells after treatment of antisense was performed by staining the cells with methylene blue. Colonies were counted using Innotech Alpha Imager HP. *$p < 0.03$, compared to respective controls

number of invading cells in the RLIP antisense-treated groups compared with controls. These findings show that the in vitro invasive ability of OC cells is inhibited by RLIP depletion (Fig. 2B).

RLIP inhibition/depletion suppresses tumor growth and metastasis in an orthotopic mouse model in vivo

Most OC patients experience the spread of OC cells to the peritoneum. Therefore, we tested whether RLIP-targeting agents could inhibit the migration of OC cells in an orthotopic mouse model. Localized cancer cells were detected in animals implanted with HeyA8-luc cells on the day following implantation (Day 1) (Fig. 3). On the next day, mice were treated with RLIP antibody (Rab) and RLIP antisense (RAS) (4 mg/kg body weight) by *i.p.* injection once a week for 7 weeks. Another group was used to compare the combined efficacy of Rab with RAS (Rab + RAS) in suppressing tumor growth and metastasis. The initial tumors in the treatment groups were noticeably smaller. After 49 days, tumor weight and tumor size in the Rab, RAS, and Rab + RAS groups were significantly reduced compared with controls. Rab and RAS caused 55% and 64% reduction in tumor size, respectively, while the Rab + RAS combination produced an 84% reduction in tumor size (Fig. 3). These results show that RLIP depletion/inhibition prevents the growth, recurrence, and metastasis of primary ovarian tumors. This finding is further supported by reduced metastasis following Rab- and RAS-induced RLIP inhibition/depletion.

As shown in Fig. 3, firefly luciferase intensity increased over time in control groups, whereas mice receiving *i.p.* RLIP-targeting agents showed much lower luciferase intensity by Day 49. NSG mice receiving RLIP-targeting agents also showed higher survival rates than controls (Fig. 3). H&E staining of primary tumor tissues from control and treated groups showed that Rab-, RAS-, and Rab + RAS-treated mice had reduced tumor growth compared with controls. Other organs examined by H&E staining, including ovary, spleen, brain, and kidney, showed no signs of toxicity in either group. Under H&E staining, metastatic foci in the liver were also lower in treated mice than in controls (Fig. 4).

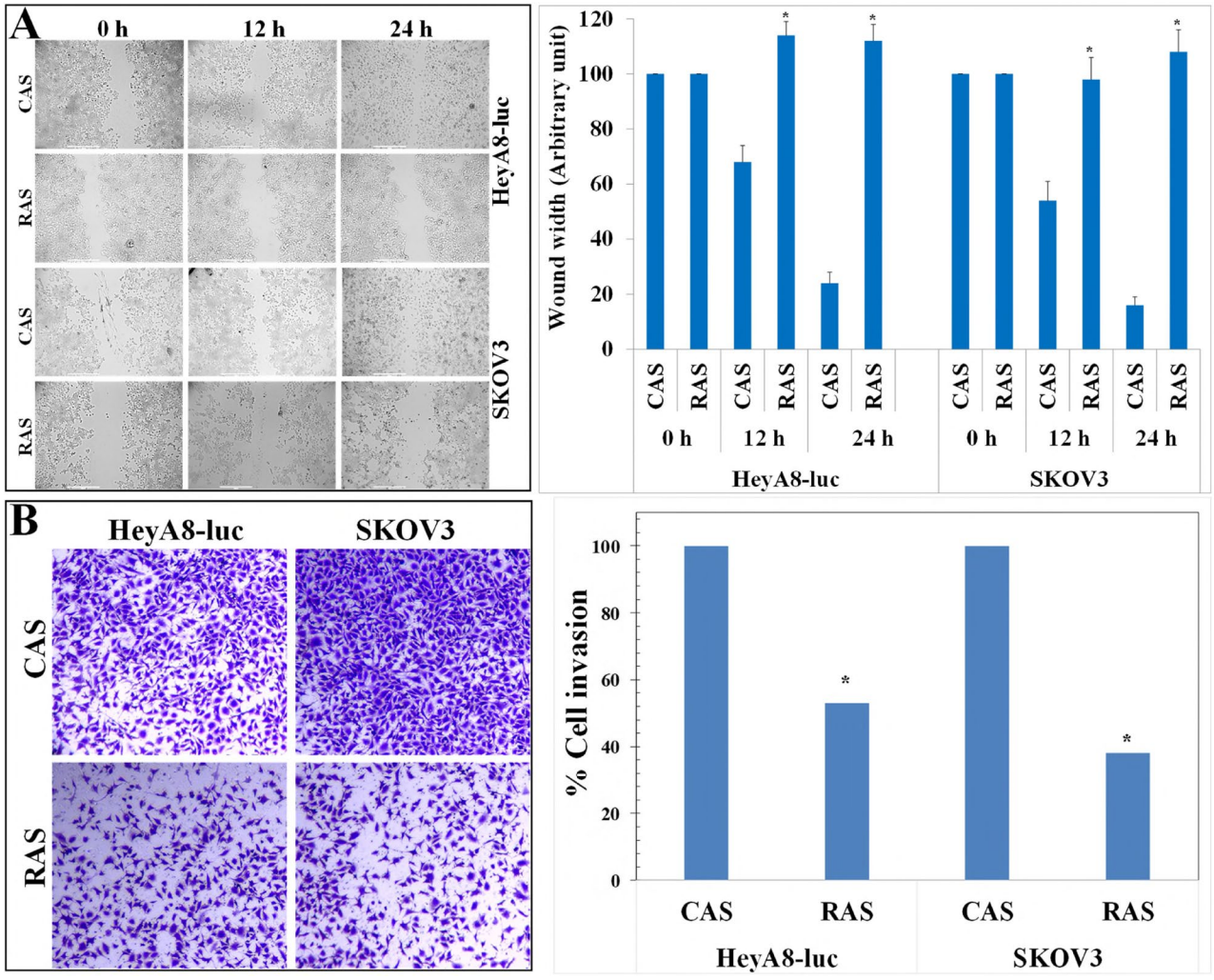

Fig. 2 Effects of RLIP depletion on the migration and invasion of OC cell lines. **A** HeyA8-luc and SKOV3 OC cells were grown to ~90% confluency in cell culture dishes. A scratch/wound was made in each dish. The cells were then treated with control scrambled (CAS) and RLIP antisense (RAS) for 24 h. Images were taken at each time point for the respective control and treatment groups. The distance across the wound was measured for three replicate experiments and quantified as the wound width. $p < 0.03$ when compared with respective controls. **B** HeyA8-luc and SKOV3 OC cells were placed in the upper chamber of the transwell inserts (8 µm pore size) in serum-free medium and then treated with either control scrambled (CAS) and RLIP antisense (RAS) for 24 h. The number of invaded cells were fixed with 4% paraformaldehyde and stained with 0.2% crystal violet. Invasive cells were then photographed under a light microscope at 200×. Quantification of invaded cells in RLIP antisense treated cells is shown after normalizing the percentage of invaded cells in control. Significantly different (*$p < 0.02$) compared with respective Controls by Student's *t* test

Immunohistochemical analysis of peritoneal tumor sections from Rab-, RAS-, and Rab + RAS-treated mice showed reduced RLIP levels, reduced Ki67 (proliferation marker), reduced CD31 (angiogenesis marker), reduced vimentin (mesenchymal marker), and increased E-cadherin (epithelial differentiation marker), whereas control sections did not show these changes (Fig. 5). In vivo RLIP expression was also reduced in antisense-treated tissues as demonstrated by immunohistochemical analysis (Fig. 6). These in vivo and in vitro findings are consistent with the observation that RLIP depletion suppresses cellular proliferation and induces programmed cell death. Overall, our results indicate that RLIP inhibition/depletion exerts strong anticancer effects on OC tumors in vivo.

Discussion

OC (epithelial ovarian, fallopian tube, as well as primary peritoneal cancer) is one of the most life-threatening gynecological tumors and is typically discovered at a later stage in its progression, which leads to poor prognosis. It is the fifth leading cancer-related death in the United States in females, with an estimated 20,890 incidences and 12,730 deaths in 2025 (American Cancer Society, Cancer Facts & Figs. 2025). Because of the unfaithfulness of screening procedures, the majority of patients show up with Stage III or Stage IV cancer, and almost a third of them have malignant ascites during the early diagnostic phase [2, 30]. The conventional methods of treatment are surgery and chemotherapy (NCCN guidelines). The

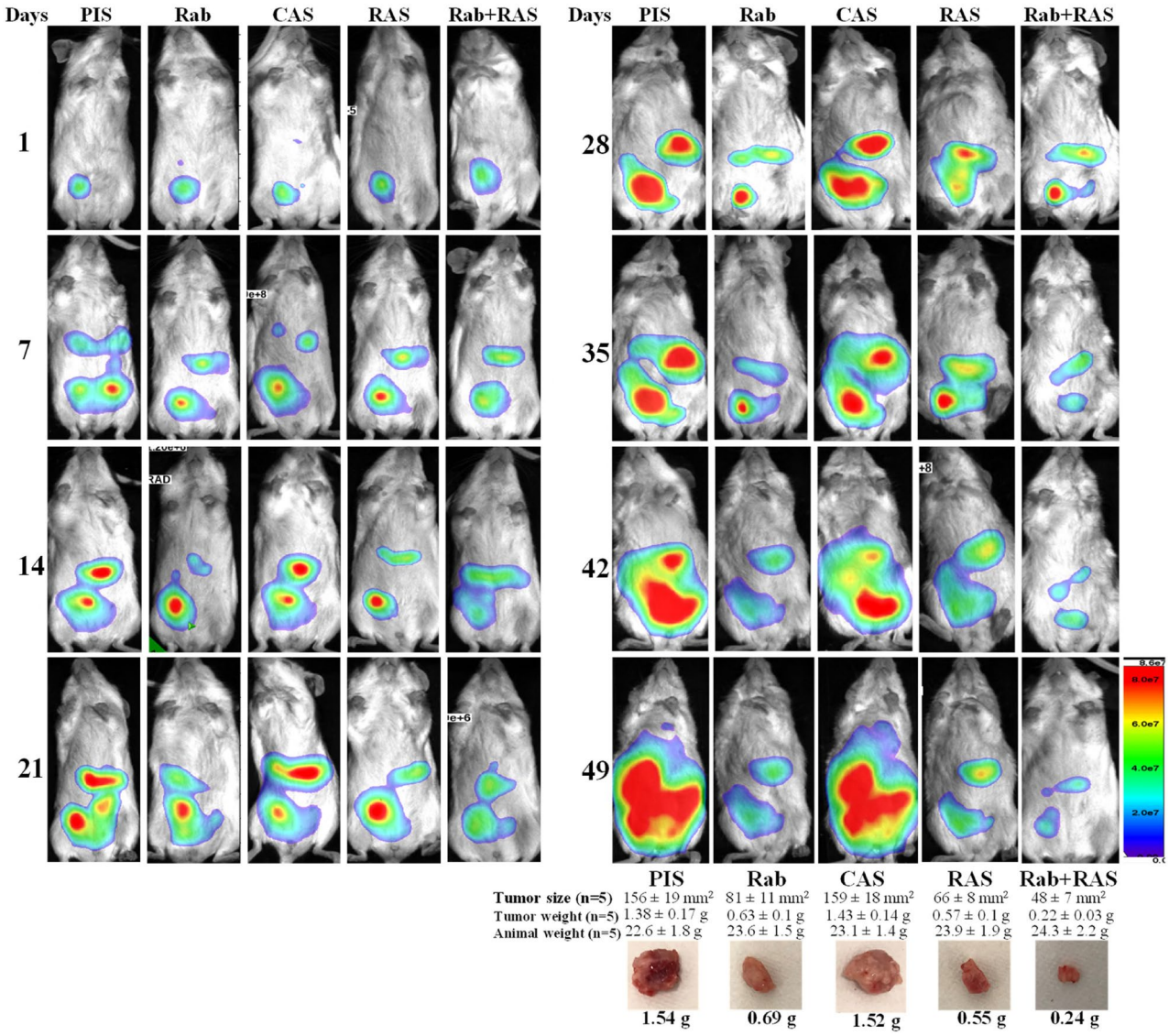

Fig. 3 Effect of RLIP-targeting agents on orthotopic mouse models of OC. HeyA8-luc OC cells were injected into the peritoneum of NSG mice ($n=5$/group), which were randomized into 5 groups (PIS, CAS, Rab, RAS, and Rab + RAS). The test group of mice received RLIP antibodies (Rab), RLIP antisense (RAS), and their combination, whereas control mice received control scrambled antisense (CAS) and pre-immune IgG (PIS) (4 mg/kg b.w. *i.p.* in saline weekly for 7 weeks). Bioluminescent in vivo imaging of animals was used to monitor metastasis twice a week after the peritoneum injection. The scale for bioluminescence intensity is shown on the right. Representative photographs of mice from each group are presented. Luminescence signal in either single agent (Rab or RAS) treated or combination (Rab + RAS) treated animal was much lower and statistically different when compared with controls (i.e., PIS or CAS treated animals), and at week 4 to week 7, the signal intensity was significantly lower ($p<0.01$) in combined (Rab + RAS) treated animals compared to single agent treated animals. Body weights were recorded weekly, and the primary tumor's cross-sectional area was measured at week 7 using caliper. Photographs of tumors were also taken in week 7

five-year general survival score in the United States is low as 49% (SEER Cancer Statistics Review). This is why there is an immediate necessity to use alternative therapeutic measures in order to cope with this life-threatening disease.

The objective of this study was to evaluate whether RLIP-targeting agents could inhibit metastatic progression of OC in a mouse model carrying a p53 mutation (HeyA8-luc-OC). RLIP, an ATPase encoded by the *ral*-binding protein-1 gene (*RALBP1*), plays a key role in the mercapturic acid pathway (MAP) and serves as a critical rate-limiting factor in clathrin-dependent endocytosis (CDE) [31]. RLIP expression is highly associated with cell migration in tumor development and is required for cancer cell metastasis [13]. To date, no oncogene knockdown has been shown to suppress spontaneous carcinogenesis in p53-null mice; however, partial pharmacological inhibition of RLIP has been reported to inhibit lymphoma and other tumors in p53-knockout mice [32]. Moreover, RLIP expression is markedly elevated in several solid

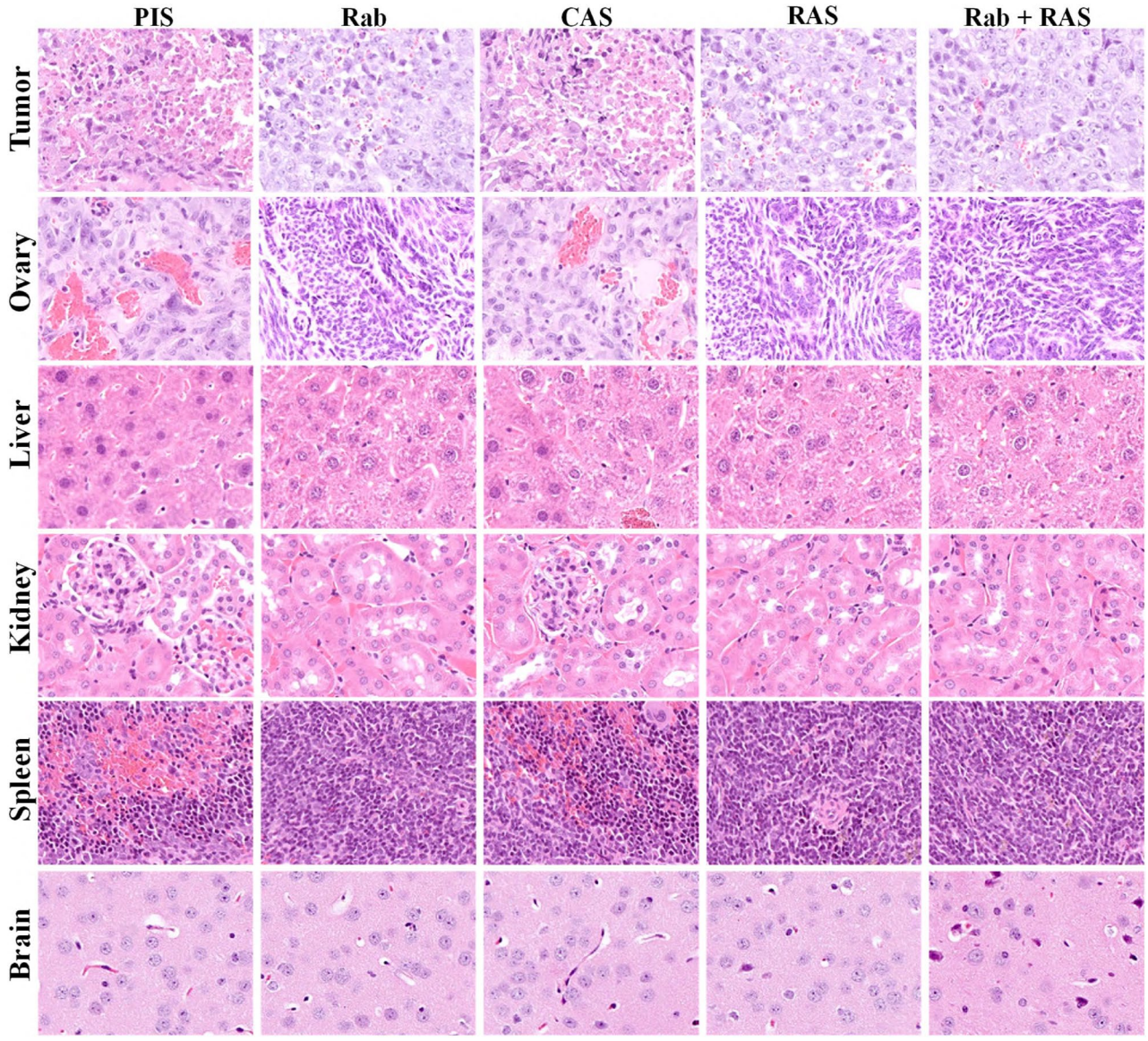

Fig. 4 Effect on the morphology of tumors and other organs excised at day 49 from HeyA8-luc OC cells injected into peritoneum of NSG mice. Control treated (PIS and CAS) and experimental treated (Rab, RAS, and Rab + RAS) groups bearing NSG mice tumors and other tissue sections were used for H&E staining. Hemorrhagic areas involving the ovary, spleen, and kidney tissues were observed in the control-treated mice, whereas tissues from experimental-treated mice were histologically normal. PIS, pre-immune serum treated; CAS, control antisense treated; Rab, RLIP antibody treated; RAS, RLIP antisense treated

tumors compared with adjacent normal tissues [11, 12, 20–25]. These observations support further investigation into RLIP inhibition/depletion as a promising strategy to suppress metastasis in an orthotopic OC model.

In this study, we tested the hypothesis that systemic suppression of RLIP using antisense oligonucleotides and/or antibody-based immunotherapy would reduce ovarian tumor growth and metastatic spread. The comparable effects produced by RLIP antisense and RLIP antibody treatment suggest that the anti-apoptotic and stress-protective functions of RLIP are largely attributable to its transport phenotype [17–19]. Overall, our results demonstrate that *i.p.* administration of RLIP-targeting agents is both feasible and effective, showing strong synergistic anticancer activity in preclinical models of OC. These findings support RLIP inhibition/depletion as a promising direction for future clinical investigation and potential therapeutic intervention in OC.

Conclusions

The omentum, located adjacent to the ovaries and rich in adipose tissue, provides a highly favorable microenvironment for OC cell proliferation and metastasis. Because

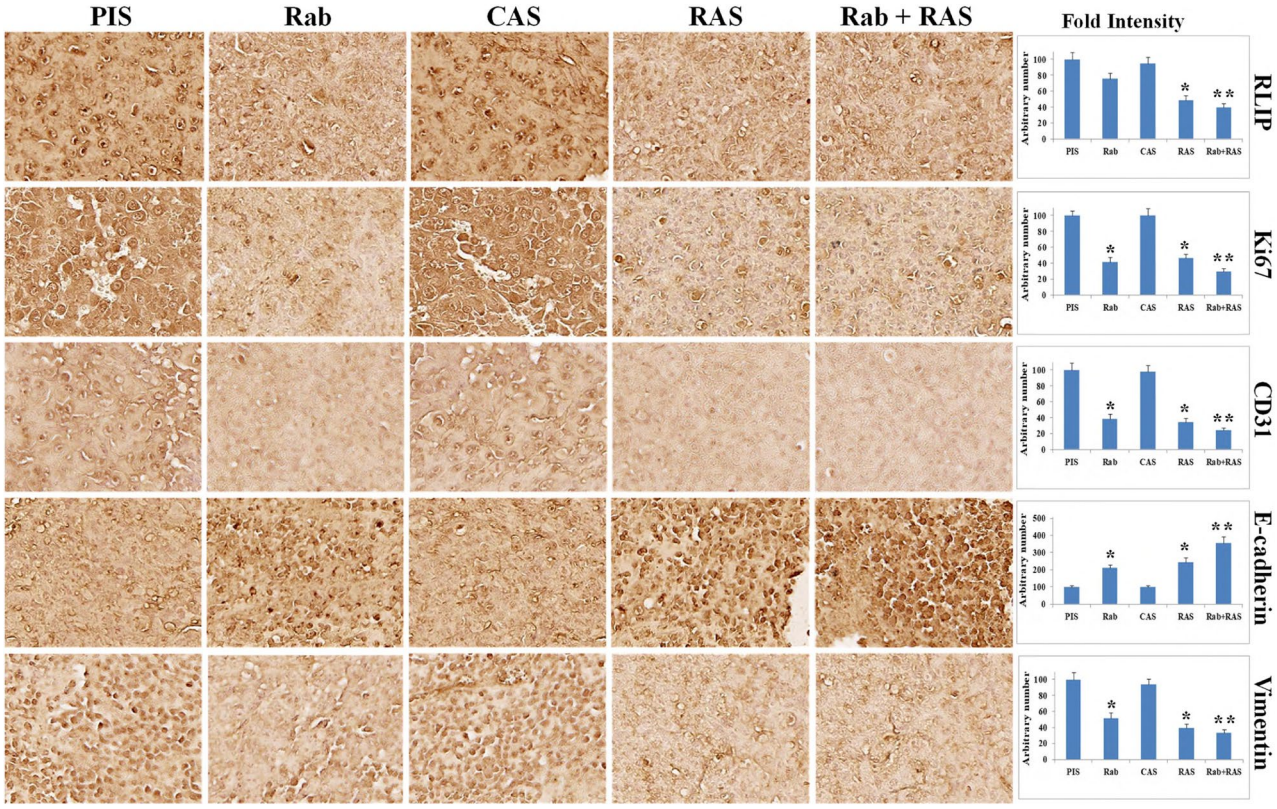

Fig. 5 Immunohistochemistry of peritoneum tumor tissue from mice in control and experimental treatment groups. Immunohistochemistry was performed to detect RLIP, Ki67, CD31, E-cadherin, and vimentin on tumor tissues isolated from control (PIS and CAS) and treatment (Rab, RAS, and Rab + RAS) groups mice at day 49. Photomicrographs at 40× magnification were acquired using an Olympus DP 72 microscope. Percent staining was determined by measuring positive immuno-reactivity per unit area. The intensity of antigen staining was quantified by digital image analysis using Pro Plus software. Bars represent mean ± S.E. ($n = 5$). One representative image for each treatment group is shown. Statistical significance of difference was determined by two-tailed Student's t test; *$p < 0.03$, Rab and RAS treatments, and **$p < 0.01$, combination treatments compared with respective controls. PIS, pre-immune serum treated; CAS, control antisense treated; Rab, RLIP antibody treated; RAS, RLIP antisense treated

OC is typically asymptomatic in early stages, dissemination throughout the peritoneal cavity is common at diagnosis. The findings of this study demonstrate the strong antineoplastic potential of RLIP inhibition or depletion in OC. Our results highlight the critical role of GS-E and xenobiotic transporters in the stress-response mechanisms that support OC cell survival.

In vivo, the combination of RLIP antisense and RLIP antibodies significantly inhibited HeyA8-luc tumor growth and metastasis in an orthotopic mouse model, with no observable toxicity to major organs. Collectively, this research establishes RLIP as a key anticancer target that functions as a multidrug transporter, an anti-apoptotic protein, and a regulator of OC cell survival. Co-delivery of RLIP antisense and RLIP antibodies shows promising therapeutic potential and warrants further investigation toward future clinical application in OC. Overall, our findings identify RLIP inhibition/depletion as a viable and potent therapeutic strategy for the management of OC, including platinum-resistant disease.

Clinical impact

According to the Centers for Disease Control and Prevention, OC remains the leading cause of death among gynecologic malignancies in the United States and is the third most common gynecologic cancer globally. It is the eighth leading cause of cancer-related mortality among women worldwide [2]. One of the most significant risk factors is increasing age, as most diagnoses occur in postmenopausal women [30]. The omentum is the most frequent site of metastasis due to its high lipid content, which supports tumor growth. Omental involvement has major implications for disease progression, treatment response, and overall prognosis. OC remains the deadliest gynecologic cancer largely because of its asymptomatic nature and the absence of reliable screening tools, resulting in approximately 70% of patients being diagnosed at advanced stages. Although chemotherapeutic agents such as paclitaxel and carboplatin are widely used, their overall effectiveness is limited. Current evidence indicates that they do not significantly improve long-term survival and are associated with toxicities and

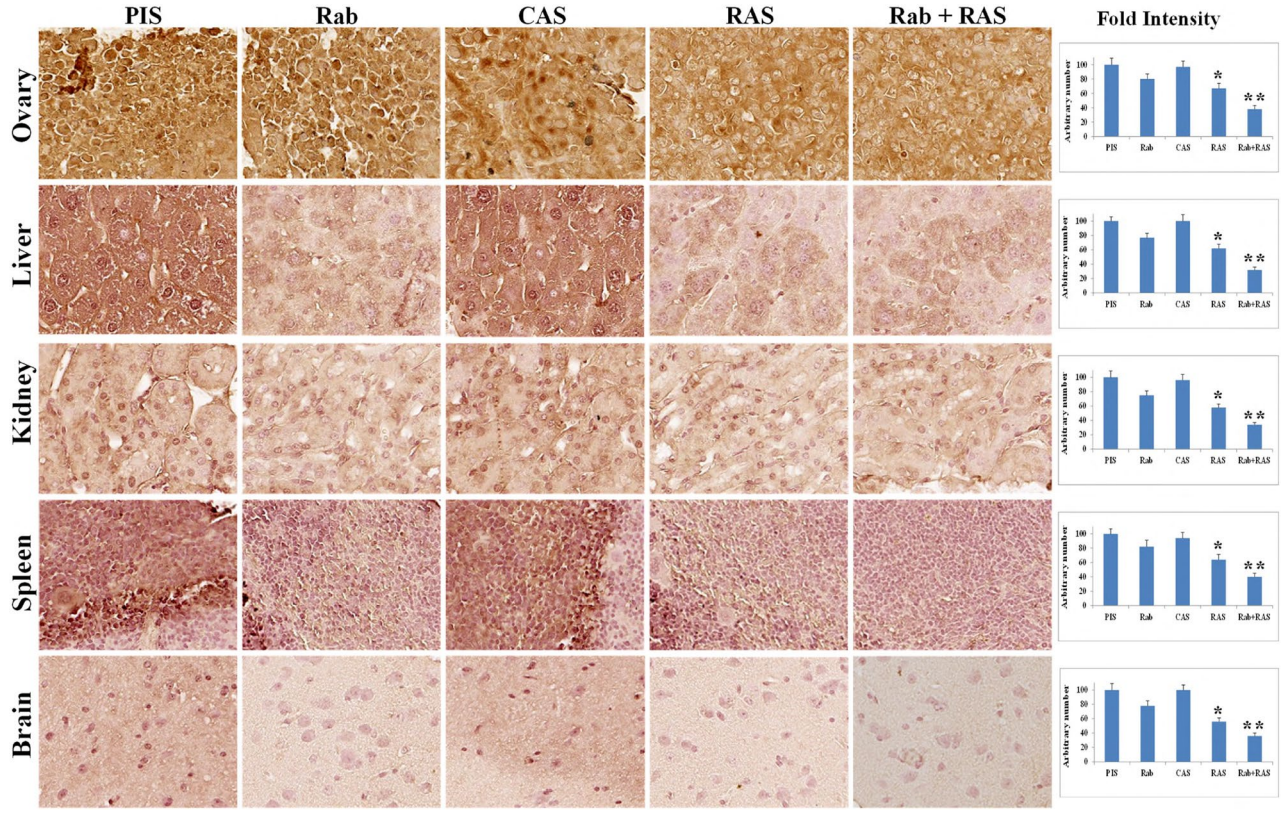

Fig. 6 Immunohistochemistry of tissues from mice in control and experimental treatment groups. Immunohistochemistry was performed to detect RLIP expression on ovary, liver, kidney, spleen, and brain tissues isolated from control (PIS and CAS) and treatment (Rab, RAS, and Rab + RAS) group mice at day 49. Photomicrographs at 40× magnification were acquired using an Olympus DP 72 microscope. Percent staining was determined by measuring positive immuno-reactivity per unit area. The intensity of antigen staining was quantified by digital image analysis using Pro Plus software. Bars represent mean ± S.E. ($n = 5$). One representative image for each treatment group is shown. Statistical significance was determined by two-tailed Student's *t* tests; *$p < 0.02$, RAS treatment, and **$p < 0.001$, Rab + RAS combination treatments compared with respective controls. PIS, pre-immune serum treated; CAS, control antisense treated; Rab, RLIP antibody treated; RAS, RLIP antisense treated

frequent development of drug resistance. This underscores the need for more selective, cancer-specific therapeutic strategies.

Our findings show that RLIP-targeting agents induce apoptosis via both intrinsic and extrinsic pathways and cause G2-cell cycle arrest by regulating cyclin B1 in OC cells. These results support the use of RLIP inhibition/depletion in platinum-resistant OC. The enhanced activity observed with the combined use of RLIP antisense and RLIP antibodies suggests a synergistic effect, potentially extending to inhibition of other ABC transporters. Thus, dual RLIP inhibition/depletion provides a significant therapeutic advantage. Future research should focus on elucidating the molecular mechanisms underlying the anti-metastatic effects of RLIP-targeting agents and evaluating their potential translation into clinical practice.

Abbreviations

CDE	Clathrin-dependent endocytosis
EOC	Epithelial ovarian cancer
GSH	Glutathione
GS-E	Glutathione-electrophile conjugate
GST	Glutathione-S-transferase
H&E	Hematoxylin and eosin staining
Luc	Luciferase
MAP	Mercapturic acid pathway
MDR	Multi-drug resistance
MRP1	Multi-drug resistance protein
MOC	Metastatic ovarian cancer
NSG	NOD scid gamma
OC	Ovarian cancer
Pgp	P-glycoprotein
PIS	Pre-immune serum
Rab	RLIP antibody
RAS	RLIP antisense
RLIP	*ral*-binding/interacting protein

Supplementary Information

The online version contains supplementary material available at https://doi.org/10.1186/s13048-026-01985-3.

Supplementary Material 1

Acknowledgements

We are grateful for the vital support provided by the staff at the Animal Research Center and the Pathology Cores. Erin Keebaugh deserves special recognition for her editorial work on this manuscript. We sincerely thank Dr.

Ravi Salgia for supporting our research and for being the Chair and Professor of the City of Hope Department of Medical Oncology.

Clinical trial number
Not applicable.

Author contributions
SSS, BMK: Contributed to data collection, analysis, interpretation, and writing the manuscript.- PG: Contributed to literature search and statistical analysis.- DH: Reviewed and edited the manuscript.- PK: Contributed to discussion and reviewed and edited the manuscript.- RS, SSS: Contributed to data interpretation and final editing.

Funding
The National Cancer Institute of the National Institutes of Health (P30CA33572) and the US Department of Defense (W81XWH-22-1-0331, HT9425-23-1-0581, and HT9425-25-1-0500) provided support for the investigation. Additionally, the Beckman Research Institute at City of Hope is acknowledged for their financial support.

Data availability
Any data created or evaluated during the current investigation can be shared by the corresponding author upon request.

Declarations

Ethics approval and consent to participate
No human participants were included in the current study. The City of Hope Animal Care and Ethics Committee approved IACUC procedure #22011 for the laboratory animal-related studies.

Consent for publication
Not applicable.

Competing interests
The authors declare no competing interests.

Received: 9 December 2025 / Accepted: 15 January 2026
Published online: 30 January 2026

References

1. Choe S, Jeon M, Yoon H. Advanced therapeutic approaches for metastatic ovarian cancer. Cancers. 2025;17:788.
2. Siegel RL, Kratzer TB, Giaquinto AN, Sung H, Jemal A. Cancer statistics. CA Cancer J Clin. 2025;75:10–45.
3. Jayson GC, Kohn EC, Kitchener HC, Ledermann JA. Ovarian cancer. Lancet. 2014;384:1376–88.
4. Veneziani AC, Gonzalez-Ochoa E, Alqaisi H, Madariaga A, Bhat G, Rouzbahman M, Sneha S, Oza AM. Heterogeneity and treatment landscape of ovarian carcinoma. Nat Rev Clin Oncol. 2023;20:820–42.
5. Webb PM, Jordan S. Global epidemiology of epithelial ovarian cancer. Nat Rev Clin Oncol. 2024;21:389–400.
6. McGuire WP, Hoskins WJ, Brady MF, Kucera PR, Partridge EE, Look KY, et al. Cyclophosphamide and cisplatin compared with paclitaxel and cisplatin in patients with stage III and stage IV ovarian cancer. N Engl J Med. 1996;334:1–6.
7. Lheureux S, Braunstein M, Oza AM. Epithelial ovarian cancer: evolution of management in the era of precision medicine. CA Cancer J Clin. 2019;69(4):280–304.
8. Yang SP, Su HL, Chen XB, Hua L, Chen JX, Hu M, Lei J, Wu S-G, Zhou J. Long-term survival among histological subtypes in advanced epithelial ovarian cancer: population-based study using the surveillance, epidemiology, and end results database. JMIR Public Health Surveill. 2021;7:e25976.
9. Konecny GE, Kristeleit RS. PARP inhibitors for BRCA1/2-mutated and sporadic ovarian cancer: current practice and future directions. Br J Cancer. 2016;115:1157–73.
10. Baldwin LA, Huang B, Miller RW, Tucker T, Goodrich ST, Podzielinski I, DeSimone CP, Ueland FR, Nagell JRV, Seamon LG. Ten-year relative survival for epithelial ovarian cancer. Obstet Gynecol. 2012;120:612–8.
11. Wang CZ, Yuan P, Xu B, Yuan L, Yang HX, Liu X. RLIP76 expression as a prognostic marker of breast cancer. Eur Rev Med Pharmacol Sci. 2015;19:2105–11.
12. Wang Q, Wang JY, Zhang XP, Lv ZW, Fu D, Lu YC, et al. RLIP76 is overexpressed in human glioblastomas and is required for proliferation, tumorigenesis and suppression of apoptosis. Carcinogenesis. 2013;34:916–26.
13. Wu Z, Owens C, Chandra N, Popovic K, Conaway M, Theodorescu D. RalBP1 is necessary for metastasis of human cancer cell lines. Neoplasia. 2010;12:1003–12.
14. Lee S, Wurtzel JGT, Goldfinger LE. The RLIP76 N-terminus binds ARNO to regulate PI 3-kinase, Arf6 and Rac signaling, cell spreading and migration. Biochem Biophys Res Commun. 2014;454:560–5.
15. Billhaq DH, Lee S. A potential function of RLIP76 in the ovarian corpus luteum. J Ovarian Res. 2019;12:34.
16. Lee S, Wurtzel J, Singhal SS, Awasthi S, Goldfinger LE. RALBP1/RLIP76 depletion in mice suppresses tumor growth by inhibiting tumor neo-vascularization. Cancer Res. 2012;72:5165–73.
17. Awasthi S, Cheng J, Singhal SS, Saini MK, Pandya U, Pikula S, et al. Novel function of human RLIP76: atp-dependent transport of glutathione conjugates and doxorubicin. Biochemistry. 2000;39:9327–34.
18. Awasthi S, Singhal SS, Sharma R, Zimniak P, Awasthi YC. Transport of glutathione conjugates and chemotherapeutic drugs by RLIP76 (*RALBP1*): a novel link between G-protein and tyrosine kinase signaling and drug resistance. Int J Cancer. 2003;106:635–46.
19. Awasthi S, Singhal SS, Yadav S, Singhal J, Drake K, Nadkar A, Zajac E, Wickrarachchi D, Rowe N, Yacoub A, et al. RLIP76 is a major determinant of radiation sensitivity. Cancer Res. 2005;65:6022–8.
20. Awasthi S, Singhal SS, Awasthi YC, Martin B, Woo J-H, Cunningham C, Frankel AE. RLIP76 and cancer. Clin Cancer Res. 2008;14:4372–7.
21. Singhal SS, Awasthi YC, Awasthi S. Regression of melanoma in a murine model by RLIP76 depletion. Cancer Res. 2006;66:2354–60.
22. Stuckler D, Singhal J, Singhal SS, Yadav S, Awasthi YC, Awasthi S. RLIP76 transports Vinorelbine and mediates drug resistance in non-small cell lung cancer. Cancer Res. 2005;65:991–8.
23. Singhal SS, Singhal J, Yadav S, Dwivedi S, Boor PJ, Awasthi YC, et al. Regression of lung and colon cancer xenografts by depleting or inhibiting RLIP76 (Ral-binding protein 1). Cancer Res. 2007;67:4382–9.
24. Singhal SS, Singhal J, Yadav S, Sahu M, Awasthi YC, Awasthi S. RLIP76: a target for kidney cancer therapy. Cancer Res. 2009;69:4244–51.
25. Ramisetty S, Garg P, Mohanty A, Mirzapoiazova T, Yue E, Wang E, et al. Regression of ovarian cancer xenografts by depleting or inhibiting RLIP. Biochem Pharmacol. 2023;217:115847.
26. Krishna BM, Ramisetty SK, Garg P, Mohanty A, Wang E, Horne D, Awasthi S, Kulkarni P, Salgia R, Singhal SS. Enhancing carboplatin sensitivity in ovarian cancer cells by blocking the mercapturic acid pathway transporter. Carcinogenesis. 2024;45:696–707.
27. Krishna BM, Garg P, Kulkarni P, Horne D, Salgia R, Singhal SS. Targeting the oncoprotein RLIP as novel therapy for ovarian cancer. J Ovarian Res. 2025;18:150.
28. Singhal SS, Roth C, Leake K, Singhal J, Yadav S, Awasthi S. Regression of prostate cancer xenografts by RLIP76 depletion. Biochem Pharmacol. 2009;77:1074–83.
29. Singhal SS, Singhal J, Sharma R, Singh SV, Zimniak P, Awasthi YC, et al. Role of RLIP76 in lung cancer doxorubicin resistance: the ATPase activity of RLIP76 correlates with doxorubicin and 4-hydroxynonenal resistance in lung cancer cells. Int J Oncol. 2003;22:365–75.
30. Sambasivan S. Epithelial ovarian cancer: review article. Cancer Treat Res Commun. 2022;33:100629.
31. Singhal SS, Wickramarachchi D, Yadav S, Singhal J, Leake K, Vatsyayan R, et al. Glutathione-conjugate transport by RLIP76 is required for clathrin-dependent endocytosis and chemical carcinogenesis. Mol Cancer Ther. 2011;10:16–28.
32. Awasthi S, Tompkins J, Singhal J, Riggs AD, Yadav S, Wu X, et al. RLIP depletion prevents spontaneous neoplasia in TP53 null mice. Proc Natl Acad Sci USA. 2018;115:3918–23.

Publisher's Note